Experimental Assessment with Wind Turbine Emulator of Variable-Speed Wind Power Generation System using Boost Chopper Circuit of Permanent Magnet Synchronous Generator

Sirichai Tammaruckwattana[*], Kazuhiro Ohyama[†], and Chenxin Yue[*]

[*†]Department of Electrical Engineering, Fukuoka Institute of Technology, Fukuoka, Japan

Abstract

This paper presents experimental results and its assessment of a variable-speed wind power generation system (VSWPGS) using permanent magnet synchronous generator (PMSG) and boost chopper circuit (BCC). Experimental results are obtained by a test bench with a wind turbine emulator (WTE). WTE reproduces the behaviors of a windmill by using servo motor drives. The mechanical torque references to drive the servo motor are calculated from the windmill wing profile, wind velocity, and windmill rotational speed. VSWPGS using PMSG and BCC has three speed control modes for the level of wind velocity to control the rotational speed of the wind turbine. The control mode for low wind velocity regulates an armature current of generator with BCC. The control mode for middle wind velocity regulates a DC link voltage with a vector-controlled inverter. The control mode for high wind velocity regulates a pitch angle of the wind turbine with a pitch angle control system. The hybrid of three control modes extends the variable-speed range. BCC simplifies the maintenance of VSWPGS while improving reliability. In addition, VSWPGS using PMSG and BCC saves cost compared with VSWPGS using a PWM converter.

Key words: Boost chopper circuit, Permanent magnet synchronous generator, Variable-speed wind generator system, Wind turbine emulator

I. INTRODUCTION

Wind power has become one of the most attractive energy resources for electricity production because it is virtually pollution free (if noise is not considered as pollution). Thus, a great deal of research has focused on the development of a new turbine design to reduce the cost of wind power and to make wind turbines economical and efficient. The investigation of wind power system involves high-performance wind turbine emulators (WTEs), particularly for the development of optimal control solutions. Several studies are being conducted on variable-speed wind generator systems that change the windmill rotational

frequency in proportion to wind velocity to utilize renewable wind energy effectively by using power generating systems [1]-[6]. The energy conversion efficiency of propeller windmills depends on wind velocity and windmill speed. Therefore, a converter connected to the generator must control the windmill speed in proportion to the wind velocity to maintain the maximum energy conversion efficiency [7].

In recent years, variable-speed wind generator systems using the PWM converter (PWM converter scheme) have been introduced [3]-[6]. PWM converter is costly because many switching devices are used, and its control system is complicated. However, the variable-speed wind generator systems using PWM converters are used for variable-speed large-capacity wind generator systems that require windmill speed control.

The supply of excitation energy with a converter is not required when a permanent magnet synchronous generator (PMSG) is used. Therefore, wind generator systems using

PMSG and a diode bridge rectifier to charge the battery are mainly operated at the rated wind velocity because the induced voltage is sufficiently high [8], [9]. These wind generator systems are low-cost converters. However, the windmill speed control is difficult to achieve because the converter cannot control the PMSG torque by itself. Furthermore, the induced voltage necessary for system interconnection cannot be obtained at low wind velocity. To date, a diode bridge rectifier scheme that realizes windmill speed control and system interconnection simultaneously at low wind velocity has not been reported.

This paper describes the experimental verification of a variable-speed wind power generation system (VSWPGS) that uses PMSG and boost chopper circuit (BCC; BCC scheme), with three speed control modes for wind velocity. The diode bridge rectifier and BCC are used as a converter. The speed control mode of low wind velocity controls the windmill speed by controlling the PMSG torque with BCC. BCC can control the generator torque by adjusting the armature current of PMSG. The speed control mode of middle wind velocity controls the windmill speed by controlling the PMSG torque with the system interconnection inverter. The system interconnection inverter can control the PMSG torque by adjusting the DC link voltage. The speed control mode over the rated wind velocity controls the windmill speed by controlling the windmill torque with the pitch angle control system. The pitch angle control system can control the windmill torque by adjusting the pitch angle. The extension of the variable-speed range is realized by using the hybrid control of three speed control modes. Consequently, system interconnection for all speed control modes is achieved.

II.   VARIABLE-SPEED WIND GENERATOR SYSTEM

A. System Configuration

Fig. 1 shows the variable-speed wind power generation system. The gearless mechanism that directly connects PMSG with the windmill without using a speed-increasing gear is realized by adopting the multipole PMSG as a generator. The windmill has a pitch angle control system. The pitch angle control system is activated beyond the rated wind velocity, and the windmill rotational speed is kept at the rated windmill speed. Under the rated wind velocity, the windmill rotational speed is controlled to maintain maximum energy conversion efficiency. The converter is connected to the PWM inverter for system interconnection through the DC link condenser. The PWM inverter supplies the power system with the active power obtained from the converter side.

B. Boost Converter Scheme

Fig. 1(a) shows the VSWPGS that uses the diode bridge

(a)   Diode bridge rectifier and boost converter.
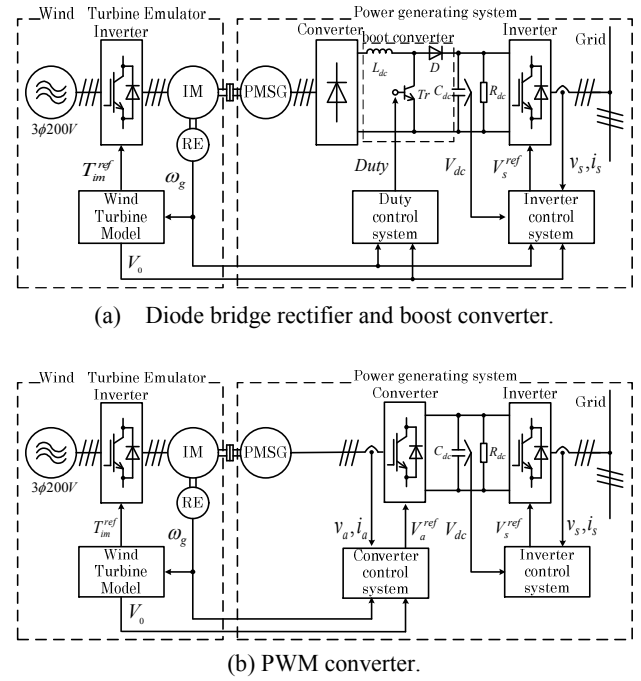

(b) PWM converter.

Fig. 1. Variable-speed wind power generator system.

rectifier and BCC (BCC scheme). The operation in the motoring mode cannot be obtained, because the diode bridge rectifier limits the current direction of the DC link. However, this condition does not become a problem, because the motoring mode is not used in this VSWPGS. The value of the DC link current depends on the relationship between the induced voltage of PMSG and the DC link voltage. Therefore, the diode bridge rectifier cannot control the generator torque. Therefore, BCC is added to improve its variable-speed range. BCC can control the DC link current regardless of the induced voltage value. In the low wind velocity range, in which the diode bridge rectifier cannot control the generator torque, BCC can control the generator torque by controlling the DC link current.

C. PWM Converter Scheme

Fig. 1(b) shows the VSWPGS that uses the PWM converter (PWM converter scheme). The PWM converter controls the windmill rotational speed by adjusting the generator torque. The PWM inverter maintains the DC link voltage to be the constant voltage necessary for the system interconnection. The PWM converter scheme can perform high-speed and high-precision generator torque control from the cut-in wind velocity to the rated wind velocity, given that the PWM converter scheme can apply the vector control system. Therefore, the frequency characteristics and variable-speed range of the windmill rotational speed control serve as a benchmark. The PWM converter scheme is referred to as a comparison object to evaluate the performance of the BCC scheme.
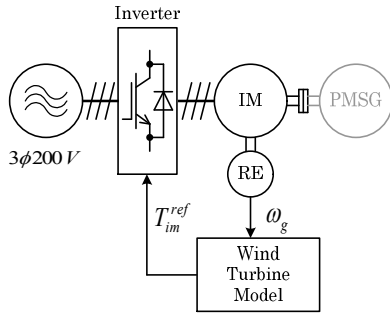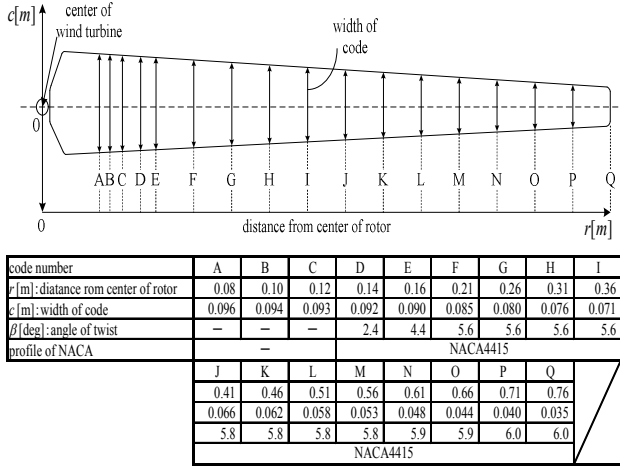
Fig. 2. WTE.

Fig. 3. Wind turbine blade shape.

code number	A	B	C	D	E	F	G	H	I
r [m] : diatance rom center of rotor	0.08	0.10	0.12	0.14	0.16	0.21	0.26	0.31	0.36
c [m] : width of code	0.096	0.094	0.093	0.092	0.090	0.085	0.080	0.076	0.071
β [deg] : angle of twist	–	–	–	2.4	4.4	5.6	5.6	5.6	5.6
profile of NACA	–					NACA4415			
	J	K	L	M	N	O	P	Q	
	0.41	0.46	0.51	0.56	0.61	0.66	0.71	0.76	
	0.066	0.062	0.058	0.053	0.048	0.044	0.040	0.035	
	5.8	5.8	5.8	5.8	5.9	5.9	6.0	6.0	
				NACA4415					

III. CONTROL SYSTEM

A. WTE

The basic structure of the WTE is shown in Fig. 2. The wind turbine model is based on blade element momentum theory (BEMT) [8]. The wind turbine model consists of three-dimensional (3D) table data of wind turbine characteristics and the mechanical model considering the difference between real wind turbine and induction motor (IM). The 3D table data are composed of the torque Q for wind velocity V_0 and windmill rotational speed ω_r. The 3D data are calculated by applying the wind turbine parameters of Fig. 3 to BEMT. V_0 is provided as a condition of emulation. ω_r is detected with the rotary encoder (RE).

c_l and c_d are obtained via fluid analysis with finite element method for each point and each meeting angle from 0° to 51°. The concrete numeric data are not given because of the space constraints. Fig. 4 shows the calculated 3D data.

B. Mechanical Model

The difference of mechanical models between real wind turbine and WTE is explained with Fig. 5. The moment of inertia and coefficient of viscosity are different between the wind turbine and IM. The differences affect the transient and steady-state responses. The differences must be compensated because wind velocity, V_0, always changes. The difference can be compensated by the following equation:
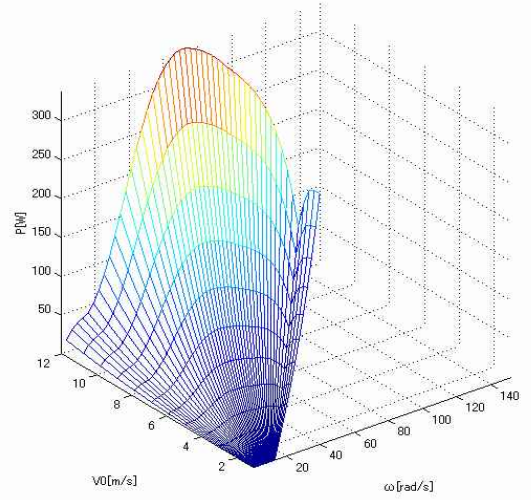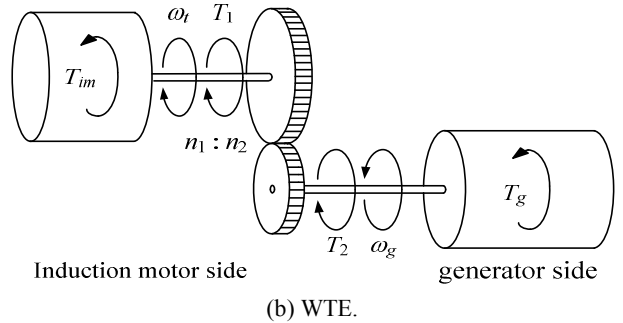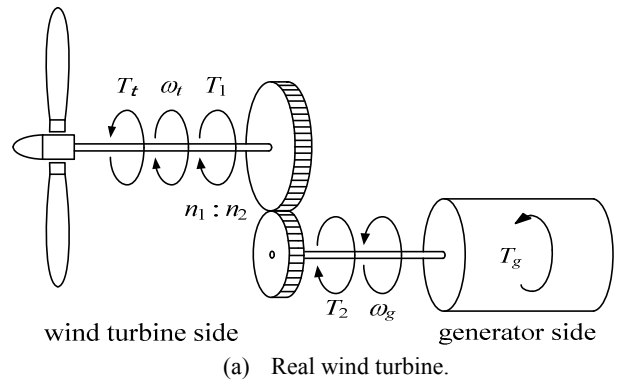

Fig. 4. 3D table data of output power.

(a)   Real wind turbine.

(b) WTE.

Fig. 5. Mechanical model.

$$T_{im}^{ref} = \frac{J_{im}}{J_t}\left(T_t - B_t\omega_t\right) + B_{im}\omega_t \tag{1}$$

where T_{im}^{ref} is the torque reference of IM [Nm], T_t is the torque of wind turbine [Nm], J_{im} is the moment of inertia for IM [kgm^2], J_t is the moment of inertia for wind turbine [kgm^2], B_{im} is the coefficient of viscosity for IM [Nm/(rad/s)], B_t is the coefficient of viscosity for wind turbine [Nm/(rad/s)], and ω_t is the rotational speed of WTE.

Fig. 6 shows the logic for the control of wind turbine and the steady state in which sufficient time has passed under the condition of fixed V_0. The timing of changing the control schemes is divided into Modes 1, 2, 3, and 4.

mode	mode 1	mode 2	mode 3	mode 4
pitch angle	fixed pitch angle (10[deg])	same	same	Vriable pitch angle
speed reference	look up table	same	ω_g^{max}	same
power reference	look up table	same	same	P^{rat}
Boost converter method	duty cycle regulator	speed regulator	same	pitch angle regulator + power regulator control with PWM inverter
PWM converter method	vector control + i_{aq} feedforwaed	same	same	pitch angle regulator + i_{aq} feedforward + power regulator control with PWM converter

Fig. 6. Logic for the control of wind turbine.
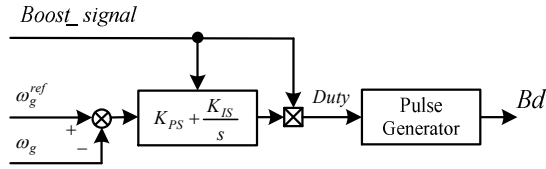
Fig. 7. Duty ratio control system for the BCC scheme.

C. Duty Control System for the BCC Scheme [9], [10]

Fig. 7 shows the duty ratio control system for BCC. The change of wind velocity includes the ranges of low wind velocity, middle wind velocity, and high wind velocity. For the low wind velocity, the duty control system adjusts the DC link current by controlling the BCC. The DC link current corresponds to the necessary generator torque to control windmill rotational speed. The DC link voltage is maintained at 35 V, which is the necessary voltage for the system interconnection by the inverter, when the duty control system is switched on. The duty becomes 0, because the DC link voltage is maintained at 35 V by the inverter, when the windmill speed rises and when the line voltage of PMSG exceeds 35 V. The operating range corresponds to a middle wind velocity. Moreover, only the rectification using the reactor and diode bridge rectifier is performed.

$$Duty = \left(K_{PS} + \frac{K_{IS}}{s} \right)\left(\omega_g^{ref} - \omega_g \right) \tag{2}$$

where K_P is the proportional gain, and K_I is the integral gain. Simulink model is constructed by Equation (2) and the pulse generator block, which estimates the B_d based on *Duty*.

D. Converter Control System for the PWM Converter Scheme

Fig. 8 shows the converter control system. In the operating range under the rated wind velocity, the speed regulator is used jointly with the torque current feed-forward control. In
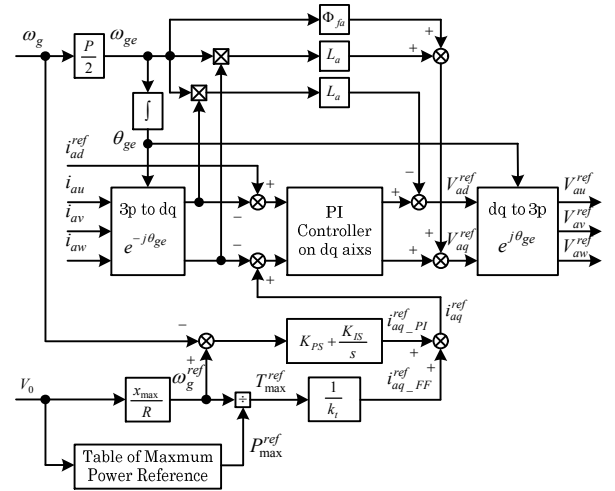

Fig. 8. Converter control system for the PWM converter scheme.

the operating range over the rated wind velocity, the pitch angle control system controls the windmill rotational speed, and the converter control system conducts the electric power control and torque current feed-forward control. The converter control system is configured by the following equations. The torque current feed-forward control is described as follows:

$$i_{aq\_FF}^{ref} = \frac{1}{P\Phi_{fa}} T_g^{ref} \tag{3}$$

Under the rated wind velocity, the rotational speed is controlled by regulating the torque current of PMSG. The torque current reference is calculated by the following equation of the PI controller:

$$i_{aq\_PI}^{ref} = \left(K_{PS} + \frac{K_{IS}}{s} \right)\left(\omega_g^{ref} - \omega_g \right) \tag{4}$$

Over the rated wind velocity, the windmill rotational speed is controlled by regulating the wind turbine torque. The wind turbine torque is regulated by the pitch angle control system as follows:

$$\theta^{ref} = \left(K_p + \frac{K_I}{s} \right)\left(\omega_g^{ref} - \omega_g \right) \tag{5}$$

Moreover, the output power is kept at the rated value by regulating the torque current of PMSG. The torque current reference is calculated by the following equation of the PI controller:

$$i_{aq\_P}^{ref} = \left(K_{PP} + \frac{K_{IP}}{s} \right)\left(P_s^{ref} - P_s \right) \tag{6}$$

The stator voltage references are calculated by the following equations:

$$V_{ad}^{ref} = \left(K_{Pad} + \frac{K_{Iad}}{s} \right)\left(i_{ad}^{ref} - i_{ad} \right) - \omega_{ge} L_a i_{aq} \tag{7}$$

$$V_{aq}^{ref} = \left(K_{Paq} + \frac{K_{Iaq}}{s} \right)\left(i_{aq}^{ref} - i_{aq} \right) + \omega_{ge} L_a i_{ad} + \omega_{ge} \Phi_{fa} \tag{8}$$

E. Inverter Control System for the BCC Scheme

Fig. 9 shows the inverter control system for the BCC scheme. The windmill speed control is performed by using the duty control system, when the induced voltage of PMSG is under 35 V. Then, the inverter control system maintains the DC link voltage at 35 V. The duty control system cannot control the windmill rotational speed when the DC link voltage exceeds 35 V. This operating range corresponds to the ranges of middle wind velocity and high wind velocity. In a middle wind velocity under the rated wind velocity, the windmill speed control is performed with the inverter control system. Concretely, the inverter control system adjusts the electric torque of PMSG by adjusting the DC link voltage, and this system controls the windmill rotational speed. In high wind velocity, in which the wind velocity exceeds the rated wind velocity, the windmill rotational speed control is performed with the pitch angle control system. Moreover, the inverter control system performs the electric power control. The inverter control system is configured by the following equations of PI speed controller:

$$V_{dc\_\omega}^{ref} = \left(K_{PS} + \frac{K_{IS}}{s} \right)\left(\omega_g^{ref} - \omega_g \right) \tag{9}$$

Over the rated wind velocity, the rotational speed is controlled by regulating the wind turbine torque. The wind turbine torque is regulated by the pitch angle control system as follows:

$$\theta^{ref} = \left(K_p + \frac{K_I}{s} \right)\left(\omega_g^{ref} - \omega_g \right) \tag{10}$$

When the pitch angle control is activated, the DC link voltage reference is calculated by the following equation of PI power controller:

$$V_{dc\_P}^{ref} = \left(K_{PP} + \frac{K_{IP}}{s} \right)\left(P_s^{ref} - P_s \right) \tag{11}$$

The DC link voltage is controlled by regulating the active current. The DC link voltage reference is calculated by subtracting outputs of PI speed and power controllers from constant DC link voltage reference:

$$i_{sd}^{ref} = \left(K_{PV} + \frac{K_{IV}}{s} \right)\left\{ V_{dc}^{ref} - \left(V_{dc\_\omega}^{ref} + V_{dc\_P}^{ref} \right) - V_{dc} \right\} \tag{12}$$

The reactive current reference is constant at 0 to keep the power factor at 1. The output voltage references are calculated by using the following equations:

$$V_{sd}^{ref} = \left(K_{Psd} + \frac{K_{Isd}}{s} \right)\left(i_{sd}^{ref} - i_{sd} \right) + e_{sd} - \omega_s L_s i_{sq} \tag{13}$$

$$V_{sq}^{ref} = \left(K_{Psq} + \frac{K_{Isq}}{s} \right)\left(i_{sq}^{ref} - i_{sq} \right) + \omega_s L_s i_{sd} \tag{14}$$
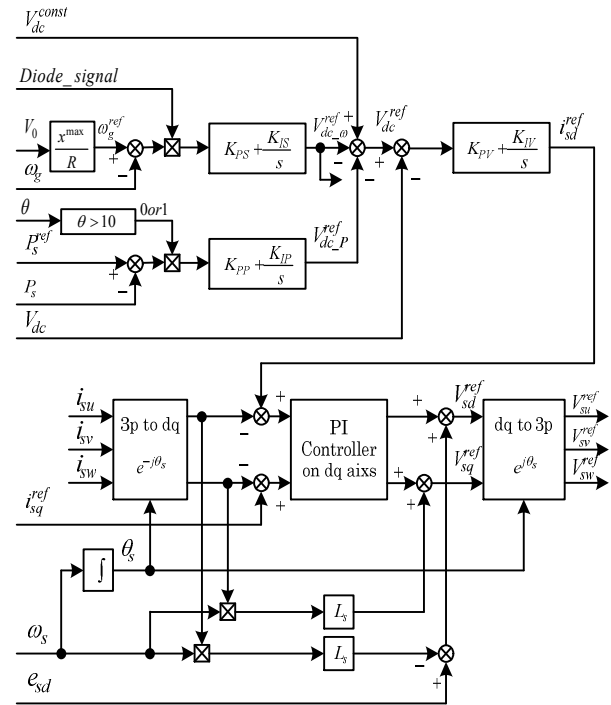

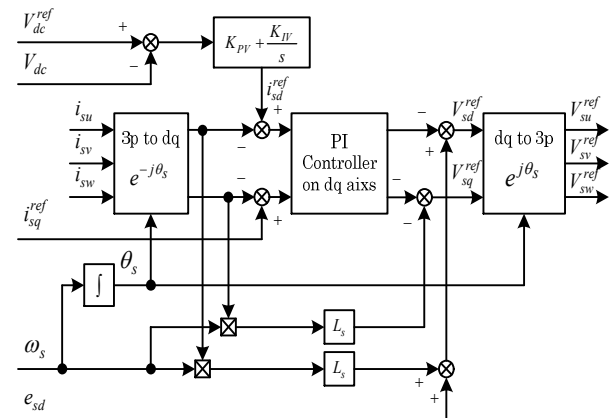
Fig. 9. Inverter control system for the BCC scheme.

Fig. 10. Inverter control system for the PWM converter scheme.

F. Inverter Control System for the PWM Converter Scheme

Fig. 10 shows the inverter control system of the PWM converter scheme. The PWM converter scheme performs the speed control and electric power control of PMSG on the converter side. In the PWM converter scheme, the DC link voltage V_{dc} is controlled at the constant of 35 V to perform speed control and electric power control of PMSG, whereas the system interconnection is conducted in the operating ranges of wind velocity. The d axis current reference i_{sd}^{ref} of Equation (12) is estimated by using the constant DC link voltage reference V_{dc}^{ref} of 35 V. Moreover, i_{sq}^{ref} is set at 0 to maintain the power factor of a power system at 1. The current controller is composed of Equations (13) and (14).
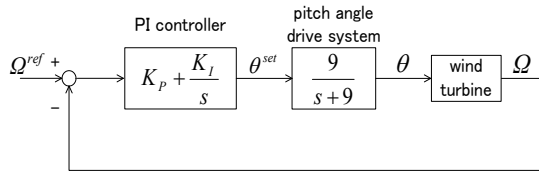
Fig. 11.− Pitch angle control system.

TABLE I

GENERATOR, POWER SYSTEM, AND TRANSFORMER PARAMETERS

Permanent Magnet Synchronous Generator	
Rated power	300[W]
Rated voltage	200[V]
Pole number	16
Stator resistance	1.419[Ω]
Stator inductance	0.4741[mH]
Mutual inductance	0.2139[mH]
Stator flux	0.07293[Wb]
Gear ratio	1
DC link	
Resistance	1000[Ω]
Capacitance	1[F]
Power system	
Line resistance	0.01[Ω]
Line inductance	0.0001[H]
Transformer	
Output:	
Type	S3P-240-10
Number of phase	3 phase
Output voltage	0 - 240[V]
Voltage fluctuation rate	5% or less
Allowable current	20[A]
Capacity	3.46[KVA]
Input:	
Input voltage	200[V]
Input frequency	50/60[Hz]

G. Pitch angle control system

Fig. 11 shows the block diagram of the pitch angle control system. The model of the pitch angle drive system describes the response of the displacement servo system and the hydraulic cylinder. This model is described as the first-order lag element, because the hydraulic cylinder has integral characteristics and because it becomes the response of the closed-loop system that comprises the servo gain. The time constant of the first-order lag element is the time constant of the pitch angle control system adopted for the wind generation system.

Table I shows the generator and power system parameters. The parameters of PMSG, power system, and transformer are common. Table II shows the control parameters for the BCC scheme. The control parameters of the boost converter and duty control system are designed with the simulations by using the implemented Simulink models. The control parameters of the vector control system applied in the inverter side are
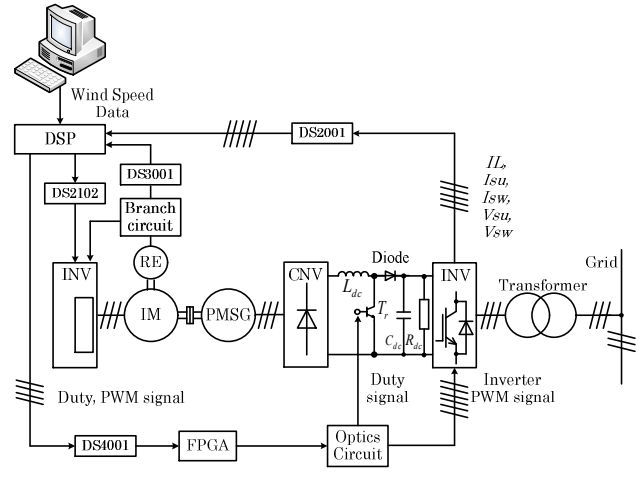
(a) BCC scheme.
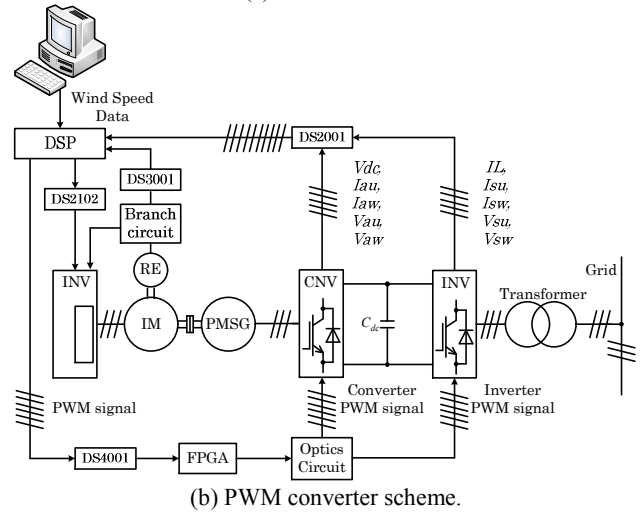
(b) PWM converter scheme.

Fig. 12. Experimental system.

designed with the conventional method that considers the arrangement of pole and zero based on the control theory. Table III shows the control parameters of the PWM converter scheme. The control parameters of the vector control system applied in the converter and inverter sides are designed with the conventional method that considers the arrangement of pole and zero.

IV. EXPERIMENTAL SYSTEM

Fig. 12 shows the experimental system of the BCC and PWM converter schemes. The digital signal processing (DSP) unit calculates the wind turbine torque reference from the wind velocity data and rotational speed of the IM. The wind velocity data are provided by the stored data in a PC. The rotational speed of IM is estimated in the DSP by using the signals from the RE. The torque of IM is controlled by the off-the-shelf inverter. The IM is operated based on the wind turbine torque reference sent from a DSP through the D/A board (DS2102). After the WTE is activated, the PMSG starts to rotate, and the converter control system starts to control the

<div style="text-align:center">

TABLE II

CONTROL PARAMETERS OF BOOST CONVERTER

</div>

Boost Convertor System	
Inductance of boost convertor circuit	1[mH]
Duty Cycle controller	
Proportional gain of speed regurator	20
Integral gain of speed regurator	100
Switching frequency	1[kHz]
Vector controller for Invertor	
Proportional gain of DC link voltage regurator	-100
Integral gain of DC link voltage regurator	-500
Proportional gain of speed regurator	1
Integral gain of speed regurator	500
Proportional gain of maxmum power regurator	0.000001
Integral gain of maxmum power regurator	0.001
Proportional gain of d axis current regurator	6.24/206
Integral gain of d axis current regurator	6.24
Proportional gain of q axis current regurator	6.24/206
Integral gain of q axis current regurator	6.24
Setting of phase voltage	100/sqrt(3)
DC link voltage reference	35
Pitch angle control	
Proportional gain of speed regurator	5
Integral gain of speed regurator	10

<div style="text-align:center">

TABLE III

CONTROL PARAMETERS OF PWM CONVERTER

</div>

PWM Cnvertor System	
Vector controller for Convertor	
Proportional gain of speed regurator	100/3.12
Integral gain of speed regurator	100
Proportional gain of maxmum power regurator	0.000001
Integral gain of maxmum power regurator	0.001
Proportional gain of d axis current regurator	225/315
Integral gain of d axis current regurator	225
Proportional gain of q axis current regurator	225/315
Integral gain of q axis current regurator	225
Setting of stator flux	0.07293
Vector controller for Invertor	
Proportional gain of DC link voltage regurator	-5
Integral gain of DC link voltage regurator	100
Proportional gain of d axis current regurator	25/357
Integral gain of d axis current regurator	25
Proportional gain of q axis current regurator	25/357
Integral gain of q axis current regurator	25
Setting of phase voltage	100/sqrt(3)
DC link voltage reference	35
Pitch angle control	
Proportional gain of speed regurator	5
Integral gain of speed regurator	10

Fig. 13. Change of wind velocity.

windmill rotational speed for the maximum power point tracking. The duty and PWM signals that control the duty and INV are sent from a DSP to the short-circuit prevention circuit through a digital IO board (DS4002). The PWM signals are sent to the CNV and INV through the optical circuit.
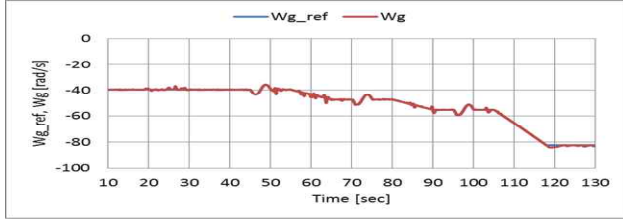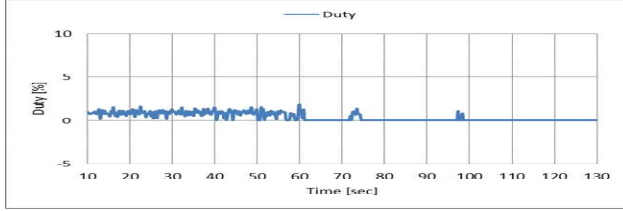
Fig. 13 shows the change of the wind velocity V_0 [m/s] and includes each mode shown in Fig. 6. The change of wind velocity includes the ranges of low wind velocity at 5 m/s, which corresponds to Mode 1, wind velocity at 6 m/s, which corresponds to the switching point between Modes 2 and 3, middle wind velocity at 7 m/s, which corresponds to Mode 2 and Mode 3, and high wind velocity at 11 m/s, which corresponds to Mode 4. High wind velocity denotes the wind velocity that exceeds the rated value. All ranges include the sinusoidal change of amplitude: 0.5 [m/s] and 0.2 [Hz]. The BCC and PWM converter schemes are tested for the same change of the wind velocity, and the control performances of both schemes are discussed.

Figs. 14 and 15 show the experimental results of the BCC scheme. The system activates at 5 m/s, which exceeds the cut-in wind velocity of 3 m/s, and the power generation started after approximately 9 seconds, in which windmill speed ω_g reaches the windmill rotational speed reference ω_g^{ref}. In the wind velocity of 5 m/s, which corresponds to Mode 1, the speed control is performed by the duty control system. Fig. 14 illustrates that windmill speed ω_g and duty can confirm that the speed control is well performed. Fig. 15 illustrates that ω_g, duty, and DC link voltage V_{dc} can confirm that the speed control is performed while the speed control system is smoothly switched at the wind velocity of 6 m/s, which corresponds to the switching point of Modes 2 and 3. At the wind velocity of 7 m/s, which corresponds to Mode 3, the speed control is performed by adjusting V_{dc} with the inverter control system. ω_g and V_{dc} can confirm that the speed control is well performed. In wind velocity of 11 m/s, which corresponds to Mode 4, the speed control is performed by pitch angle control system, and the electric power control is conducted by the inverter control system. Fig. 15 illustrates that ω_g, V_{dc}, and pitch angle θ can confirm that ω_g is controlled at the rated speed and that the generated power P_s is controlled at the rated power of 300 W.
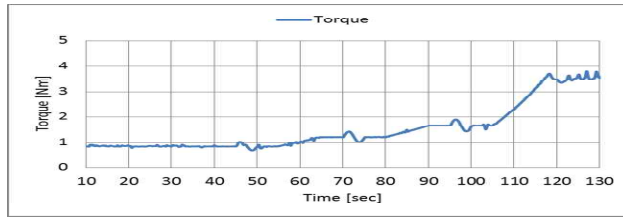
Figs. 16 and 17 show the simulation results of the PWM converter scheme. The system activates at the wind velocity of 5 m/s, which exceeds the cut-in wind velocity of 3 m/s. Moreover, the power generation started after approximately 11
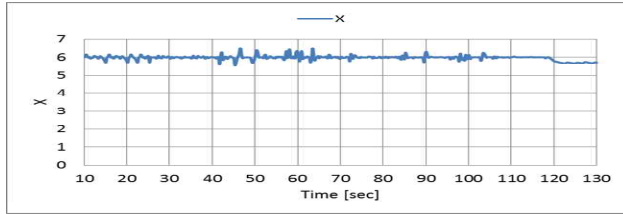
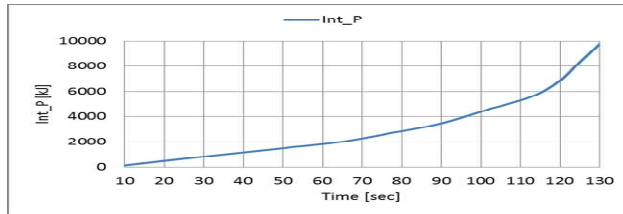(a) Rotational speed reference and rotational speed.

(a) DC link voltage and its reference.

(b) Duty control signal.

(b) System power.

(c) Wind turbine torque.

(c) Pitch angle control.

(d) Tip speed ratio.

(d) d axis and q axis current.

(e) Integrated power system.

Fig. 14. Experimental results of the BCC scheme.

(e) d axis and q axis voltage.

Fig. 15. Experimental results of the BCC scheme.

seconds, in which ω_g reaches in ω_g^{ref} as well as the BCC scheme. The system is operated under the rated wind velocity, which corresponds to Modes 1 to 3 until about 115 seconds. Thus, ω_g follows ω_g^{ref}. However, the response of the PWM converter scheme has been retarded because the increase of ω_g^{ref} corresponds to the increase of wind velocity given that the restriction of torque current reference i_{aq}^{ref} has been established so that PMSG may not conduct the motoring. The operating range, which exceeds the rated wind velocity and corresponds to Mode 4, starts after 115 seconds. The pitch angle control system starts around 118 seconds. Then, the speed controller of converter control system stops

simultaneously, and the maximum electric power tracking control is activated. The sinusoidal change of wind velocity is superimposed in this operating range. ω_g is maintained at the rated speed-by-speed control by pitch angle control system and the electric power control by converter control system. Moreover, the generated output P_s is maintained at the rated power of 300 W.

Table IV shows the integrated powers of each mode of the BCC and PWM converter schemes. Integrated P_s of the BCC scheme decreases at 0 seconds to 55 seconds, which corresponds to Mode 1, compared with integrated P_s of the PWM converter scheme, because the tracking characteristic
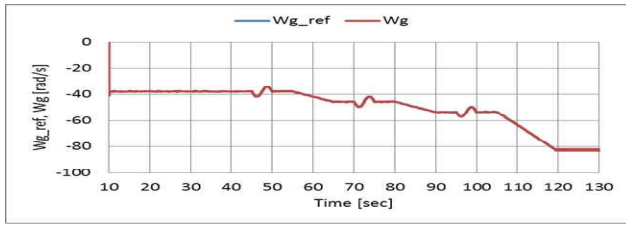
(a) Rotational speed reference and rotational speed.
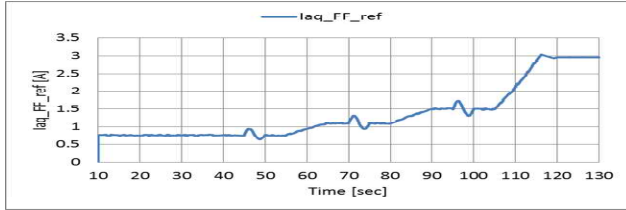
(b) *q*-axis current reference of feed-forward control.
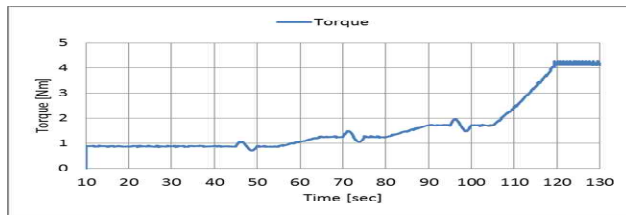
(c) Wind turbine torque.

(d) Tip speed ratio.

(e) Integrated power system.

Fig. 16. Experimental result of the PWM converter scheme.

(a) DC link voltage and its reference.

(b) System power.

(c) Pitch angle control.

(d) *d* axis and *q* axis current for converter side.
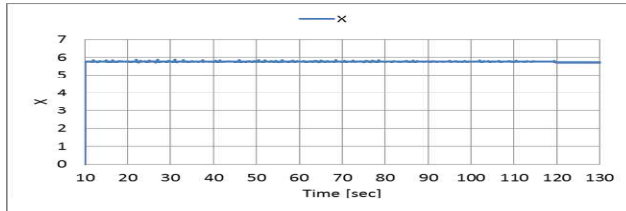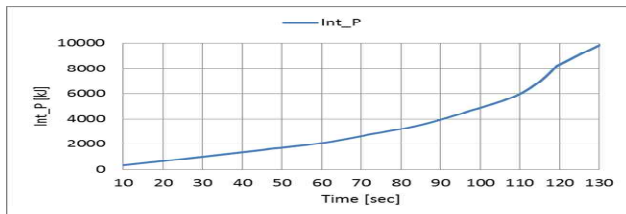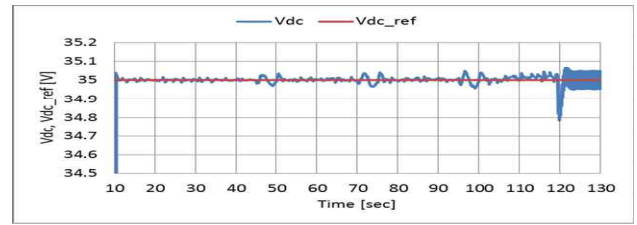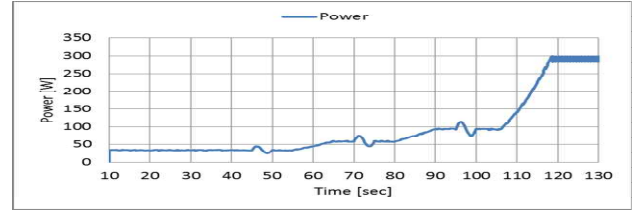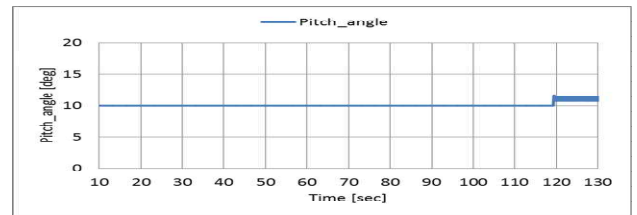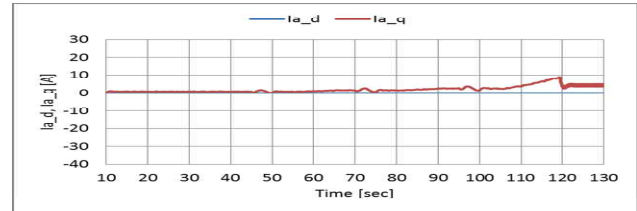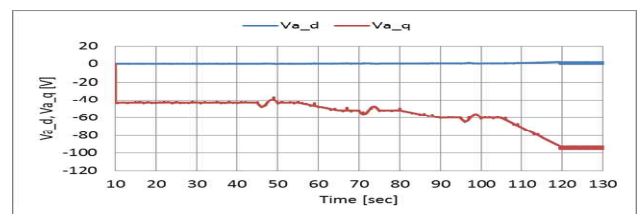

(e) *d* axis and *q* axis voltage.

Fig. 17. Experimental result of the PWM converter scheme.

of ω_g for ω_g^{ref} is inferior. The BCC scheme uses the hybrid control of the duty control system and speed control of the inverter side at 55 seconds to 80 seconds, which corresponds to the switching point of Modes 1 and 2. In this operating range, integrated P_s of the BCC scheme decreases, because the tracking characteristic of the speed reference is inferior to the PWM converter scheme. The BCC scheme charges the DC link condenser at 80 seconds to 105 seconds, which corresponds to Mode 3. Therefore, integrated P_s decreases. In this period, speed control is performed by charging the DC link condenser, given that the wind velocity increases. Integrated P_s of the BCC scheme and the PWM converter

TABLE IV
INTEGRATED POWER OF EACH MODE

Mode	Time[sec]	Integrated electric power in kJ for Boost Converter system	Integrated electric power in kJ for PWM Converter system
mode1	0-55[sec]	0-1647	0-1859
mode1 or mode2	55-80[sec]	1647-2861	1859-3197
mode3	80-105[sec]	2861-4817	3197-5344
mode4	105-130[sec]	4817-9785	5344-9813

scheme have a significant difference, given that the DC link capacitor of the BCC scheme discharges in the operating range of 105 seconds to 130 seconds, which exceeds the rated wind velocity and corresponds to Mode 4. At this operating

range, the pitch angle control is activated, and the efficiency of the converter of the BCC scheme changes because the operating circuit changes for the operating modes.

V. Conclusions

This paper proposed the VSWPGS using the BCC scheme. An implementation process that considers all systems for the BCC scheme was proposed to verify the validity. In addition, the implementation process of the VSWPGS using the PWM converter scheme was described as the benchmark comparison. The experimental systems of both schemes were built to evaluate the performance of the BCC scheme. The BCC scheme enabled windmill rotational speed control from the cut-in wind velocity to the overrated wind velocity. Therefore, the BCC scheme obtained a performance similar to that of the PWM converter scheme. The developed WTE can be used to analyze various mechanical and electrical characteristics of a grid-tied PMSG wind power system. Moreover, it can be used to educate students or engineers to understand the operation of grid-tied PMSG wind power systems.

References

[1] B. Wu, Y. Lang, N. Zargari, and S. Kouro, *Power Conversion and Control of Wind Energy Systems*, Hoboken NJ: Wiley, 2011.

[2] M. P. Kazmierkowski, R. Krishnan, and F. Blaabjerg, *Control in Power Electronics-Selected Problems*, New York: Academic Press, 2002.

[3] K. H. Kim, Y. C. Jeung, D. C. Lee, and H. G. Kim, "Robust control of PMSG wind turbine systems with back-to-back PWM converters," *IEEE International Symposium on Power Electronics for Distributed Generation Systems*, 2012.

[4] S. Li, T. A. Haskew, R. P. Swatloski, and W. Gathings, "Optimal and direct-current vector control of direct-driven PMSG wind turbines," *IEEE Trans. Power Electron.*, Vol. 27, No. 5, pp. 2325-2337, May 2012.

[5] F. Kendouli, K. Abed, K. Nabti, H. Benalla, and B. Azoui, "High performance PWM converter control based PMSG for variable speed wind turbine," *International Conference on Renewable Enegies and Vehicular Technology*, pp. 502-507, 2012.

[6] S. Tammaruckwattana and K. Ohyama, "Experimental verification of variable speed wind power generation system using permanent magnet synchronous generator by wind turbine emulator," in *Proc. IECON*, pp. 5827-5832, 2012.

[7] D. M. Eggleston and F. S. Stoddard, *Wind Turbine Engineering Design*, Springer, pp. 15-64, 1987.

[8] K. Ohyama and T. Nakashima, "Wind turbine emulator using wind turbine model based on blade element momentum theory," *International Symposium on Power Electronics, Electrical Drives, Automation and Motion T. SPEEDAM*, pp. 762-765, 2010.

[9] S. Tammaruckwattana and K. Ohyama, "Modeling and simulation of permanent magnet synchronous generator wind power generation system using boost converter circuit," in *Proc. EPE*, pp. 1-10, 2013.

[10] S. Tammaruckwattana and K. Ohyama, "Experimental verification of variable speed wind power generation system using permanent magnet synchronous generator by boost converter circuit," in *Proc. IECON*, pp. 7157-7162, 2013.

Sirichai Tammaruckwattana received his B.Eng. and M.Eng. in Electrical and Control Engineering from King Mongkut's Institute of Technology Ladkrabang, Bangkok, Thailand, in 2001 and 2005, respectively. In December 2005, he joined the Department of Control and Mechatronic Engineering, King Mongkut's Institute of Technology Ladkrabang, Bangkok, Thailand, as a lecturer. He is currently working toward a Ph.D. degree at the Department of Electrical Engineering, Fukuoka Institute of Technology, Fukuoka, Japan. He is currently engaged in research on variable speed wind power generation system using permanent magnet synchronous generator by natural wind.

Kazuhiro Ohyama received his B.Eng. in Electrical Engineering and his M.Eng. and D.Eng. from Kagoshima University, Kagoshima, Japan, in 1993, 1995, and 1998, respectively. He was a visiting scholar at the University of Nottingham, Nottingham, U.K., from 1998 to 1999. In April 1999, he joined the Department of Electrical Engineering, Fukuoka Institute of Technology, Fukuoka, Japan, as a lecturer. In April 2002, he was promoted to associate professor. Then, in April 2009, he was promoted to professor. He is currently engaged in the study of AC motor drives.

Chenxin Yue received his B.Eng. in Electrical Engineering from the Nanjing University of Science and Technology, Nanjing, China, in 2012. He is currently working toward his master's degree at the Department of Electrical Engineering, Fukuoka Institute of Technology, Fukuoka, Japan. He is currently engaged in research on variable speed wind power generation system.